

UCLA

UCLA Previously Published Works

Title

Effects of gene dosage and development on subcortical nuclei volumes in individuals with 22q11.2 copy number variations.

Permalink

<https://escholarship.org/uc/item/8g23h7w0>

Journal

Neuropsychopharmacology, 49(6)

Authors

Schleifer, Charles

O'Hora, Kathleen

Fung, Hoki

et al.

Publication Date

2024-05-01

DOI

10.1038/s41386-024-01832-3

Peer reviewed

ARTICLE OPEN



Effects of gene dosage and development on subcortical nuclei volumes in individuals with 22q11.2 copy number variations

Charles H. Schleifer^{1,2}✉, Kathleen P. O'Hora¹, Hoki Fung¹, Jennifer Xu¹, Taylor-Ann Robinson¹, Angela S. Wu¹, Leila Kushan-Wells¹, Amy Lin¹, Christopher R. K. Ching³ and Carrie E. Bearden^{1,4}✉

© The Author(s) 2024

The 22q11.2 locus contains genes critical for brain development. Reciprocal Copy Number Variations (CNVs) at this locus impact risk for neurodevelopmental and psychiatric disorders. Both 22q11.2 deletions (22qDel) and duplications (22qDup) are associated with autism, but 22qDel uniquely elevates schizophrenia risk. Understanding brain phenotypes associated with these highly penetrant CNVs can provide insights into genetic pathways underlying neuropsychiatric disorders. Human neuroimaging and animal models indicate subcortical brain alterations in 22qDel, yet little is known about developmental differences across specific nuclei between reciprocal 22q11.2 CNV carriers and typically developing (TD) controls. We conducted a longitudinal MRI study in a total of 385 scans from 22qDel ($n = 96$, scans = 191, 53.1% female), 22qDup ($n = 37$, scans = 64, 45.9% female), and TD controls ($n = 80$, scans = 130, 51.2% female), across a wide age range (5.5–49.5 years). Volumes of the thalamus, hippocampus, amygdala, and anatomical subregions were estimated using FreeSurfer, and the linear effects of 22q11.2 gene dosage and non-linear effects of age were characterized with generalized additive mixed models (GAMMs). Positive gene dosage effects (volume increasing with copy number) were observed for total intracranial and whole hippocampus volumes, but not whole thalamus or amygdala volumes. Several amygdala subregions exhibited similar positive effects, with bi-directional effects found across thalamic nuclei. Distinct age-related trajectories were observed across the three groups. Notably, both 22qDel and 22qDup carriers exhibited flattened development of hippocampal CA2/3 subfields relative to TD controls. This study provides novel insights into the impact of 22q11.2 CNVs on subcortical brain structures and their developmental trajectories.

Neuropsychopharmacology (2024) 49:1024–1032; <https://doi.org/10.1038/s41386-024-01832-3>

INTRODUCTION

Genomic copy number variations (CNVs) at the 22q11.2 locus strongly increase risk for neurodevelopmental and psychiatric disorders including autism and schizophrenia [1]. 22q11.2 Deletion Syndrome (22qDel) and 22q11.2 Duplication Syndrome (22qDup) result from reciprocal CNVs that involve hemizygous deletion or duplication of approximately 2.6 Megabases (Mb) of genomic material from the long arm of chromosome 22. The brain and behavioral phenotypes resulting from these related CNVs provide a valuable genetics-first framework for investigating biological pathways relevant to brain development and neuropsychiatric disorders [2, 3].

22qDel (OMIM #188400, #192430) is one of the strongest known genetic risk factors for schizophrenia, with over 1 in 10 individuals with 22qDel having a comorbid psychotic disorder and over one-third experiencing subthreshold psychosis symptoms [4, 5]. 22qDel also increases risk for autism, attention-deficit hyperactivity disorder (ADHD), intellectual disability, and anxiety disorders [6–8]. This microdeletion occurs in approximately 1 in 4000 people [9].

A duplication of this same region causes 22qDup (OMIM #608363) and is often inherited, unlike 22qDel which typically

arises de novo [10]. 22qDup was discovered more recently than 22qDel and has not yet been as deeply characterized [11, 12]. Individuals with 22qDup experience higher rates of neurodevelopmental disorders, including intellectual disability and autism, compared to the general population; however, the duplication generally has a milder impact on neurodevelopment compared to 22qDel [1, 13]. In contrast to 22qDel, 22qDup is *less* common in individuals with schizophrenia compared to the general population, suggesting a potential protective effect against schizophrenia in 22qDup [14–16].

In addition to widespread cortical anomalies, including reductions in surface area, concomitant with relatively increased cortical thickness [17, 18], studies of 22qDel have consistently identified structural and functional alterations in subcortical structures. A large multi-site, cross-sectional study from the ENIGMA 22q11.2 Working Group found decreased subcortical volumes in 22qDel compared to TD controls, with larger effects in those with psychosis [19]. These subcortical brain structures play key roles in cognitive, sensory, and affective processes [20]. Individual differences in subcortical anatomy have been related to both common and rare genetic variation [21, 22], and to psychiatric and

¹Department of Psychiatry and Biobehavioral Sciences, Semel Institute for Neuroscience and Human Behavior, University of California, Los Angeles, CA, USA. ²David Geffen School of Medicine, University of California, Los Angeles, CA, USA. ³Imaging Genetics Center, Mark and Mary Stevens Institute for Neuroimaging and Informatics, Keck School of Medicine, University of Southern California, Marina del Rey, CA, USA. ⁴Department of Psychology, University of California, Los Angeles, CA, USA.

✉email: cschleifer@mednet.ucla.edu; cbearden@mednet.ucla.edu

Received: 2 November 2023 Revised: 16 January 2024 Accepted: 12 February 2024

Published online: 2 March 2024

Table 1. Baseline demographics.

	TD	22qDel	22qDup	p-value
<i>n</i>	80	96	37	
Age, mean (SD)	14.89 (7.34)	15.52 (7.62)	17.83 (13.50)	0.24
Sex, <i>n</i> (%) Female	41 (51.3)	51 (53.1)	17 (45.9)	0.759
Full Scale IQ, mean (SD)	111.27 (19.28)	78.65 (12.74)	95.44 (17.84)	<0.001
SIPS Positive total, mean (SD)	1.23 (1.88)	5.86 (6.52)	2.96 (3.25)	<0.001
Psychosis Risk Symptoms, <i>n</i> (%)	4 (5.0)	24 (25.0)	5 (13.5)	0.002
Psychotic Disorder, <i>n</i> (%)	0 (0.0)	8 (8.3)	0 (0.0)	0.022
ADHD, <i>n</i> (%)	5 (6.2)	41 (42.7)	14 (37.8)	<0.001
Autism, <i>n</i> (%)	0 (0.0)	45 (46.9)	15 (40.5)	<0.001
Antipsychotic Med, <i>n</i> (%)	0 (0.0)	11 (11.5)	2 (5.4)	<0.001
Visit count, mean (SD)	1.62 (0.89)	1.99 (1.16)	1.73 (0.93)	0.058
Days between visits, mean (SD)	667.68 (546.90)	676.78 (383.58)	483.15 (111.84)	0.26
Visit 1 Prisma scanner, <i>n</i> (%)	25 (31.2)	23 (24.0)	16 (43.2)	0.090
Visit 2 Prisma scanner, <i>n</i> (%)	8 (22.9)	16 (29.6)	16 (100.0)	<0.001
Visit 3 Prisma scanner, <i>n</i> (%)	4 (36.4)	13 (46.4)	10 (100.0)	0.005
Visit 4–6 Prisma scanner, <i>n</i> (%)	4 (100.0)	15 (100.0)	1 (100.0)	NA

TD controls, 22qDel, and 22qDup with *p*-values for between group comparisons (ANOVA for continuous variables and chi-squared for categorical). Baseline cohorts are statistically matched based on age and sex as well as mean number of longitudinal visits and interval between visits. Cognition was measured with the Wechsler Abbreviated Scale of Intelligence-2 (WASI-2). Prodromal (psychosis-risk) symptoms were assessed with the Structured Interview for Psychosis-Risk Syndromes (SIPS). Psychosis Risk Symptoms are operationalized here as having any score of 3 or greater (i.e., prodromal range) on any SIPS positive symptom item. Psychotic disorder diagnosis is based on structured clinical interview (SCID) for DSM-IV/V and includes schizophrenia, schizoaffective disorder, brief psychotic disorder, and psychotic disorder not otherwise specified. The number and percentage of each group scanned on the Siemens Prisma scanner (versus Siemens Tim Trio) is reported at each time point.

neurodevelopmental disorders including schizophrenia, autism, and ADHD [23, 24].

While most of the literature to date has investigated whole subcortical structures and/or voxel-wise shape differences, these structures are composed of many small distinct nuclei [20, 25]. More recent studies have begun to investigate volumes of specific anatomical subregions of structures such as the thalamus and hippocampus. Bi-directional effects on FreeSurfer-derived thalamic nuclei volumes have been observed in 22qDel, wherein volumes of subregions involved in sensory processes (e.g., medial geniculate) were found to be smaller than controls, while subregions involved in cognitive processes (e.g., anteroventral) were larger [26]. Longitudinally, there were steeper thalamic volume decreases over time in individuals with 22qDel who experienced auditory hallucinations. In 22qDel, lower hippocampal tail volume has been related to verbal learning impairments [27], and hippocampal volume loss over time in 22qDel has been linked to altered local balance of excitatory and inhibitory neurotransmitter metabolites [28].

Few studies have directly compared brain phenotypes in 22qDel and 22qDup. In the first study comparing regional brain volumes of reciprocal 22q11.2 CNV carriers to typically developing (TD) controls, in a cross-sectional sample, our group found that gene dosage (i.e., the number of copies of the 22q11.2 locus) was positively related to cortical surface area (22qDel < TD < 22qDup) and negatively related to cortical thickness (22qDel > TD > 22qDup) [18]. This study also found larger hippocampal volumes in 22qDup relative to 22qDel, and radial thickness differences in subcortical structures, including the thalamus and amygdala. Recently, a large study of subcortical volumes in 11 different CNVs found convergent evidence for hippocampal volume differences in 22qDel versus 22qDup [21].

No study has assessed subcortical subregional volumes or longitudinal subcortical development in 22qDup, nor directly compared subregion-level volumes between 22qDup and 22qDel. Studies of subcortical shape show complex alterations in 22q11.2 CNV carriers compared to controls, with localized volume

increases and decreases suggesting differential vulnerabilities across subregions [19, 21]. Mapping gene dosage effects to functionally and histologically defined nuclei can facilitate causal links between macro-scale MRI brain signatures and cellular and molecular mechanisms inferred from other data sources including post-mortem brain tissue [29, 30], and animal models [31]. Examples of genes in the 22q11.2 locus that have been related to cortical structural phenotypes and which may have broad or region-specific effects on subcortical development include *DGCR8*, a gene involved in microRNA regulation, and *AIFM3*, a gene involved in apoptosis pathways [32].

In this longitudinal structural MRI study of reciprocal 22q11.2 CNV carriers and TD controls, across a wide age range (ages 5.5–49.5), we present the first investigation of the effects of gene dosage at the 22q11.2 locus on anatomical subregion volumes in the thalamus, hippocampus, and amygdala. We also characterize, for the first time, developmental trajectories of these subcortical volumes in individuals with 22q11.2 CNVs.

METHODS

Participants

The total longitudinal sample consisted of 385 scans from 213 participants (5.5–49.5 years of age; *n* = 96 22qDel baseline; *n* = 37 22qDup baseline; *n* = 80 TD controls baseline; see Table 1, and Fig. S1). Participants had data from 1–6 timepoints separated by an average of approximately 1.75 years. The groups were matched on baseline age and sex, mean number of longitudinal visits, and interval between visits. See Supplementary Methods for details on inclusion/exclusion criteria and clinical assessment. After study procedures had been fully explained, adult participants provided written consent, while participants under the age of 18 years provided written assent with the written consent of their parent/guardian. The UCLA Institutional Review Board approved all study procedures and informed consent documents.

Neuroimaging acquisition/preprocessing. All participants were imaged at the UCLA Center for Cognitive Neuroscience on either a Siemens TimTrio

Table 2. Gene dosage effects on subcortical volumes.

Structure	Region	beta	p	FDR q	sig
whole brain	total ICV	0.28	1.3e-03	0.0038	*
whole volumes	whole thalamus	-0.03	7.0e-01	0.8	
	whole amygdala	0.14	8.7e-02	0.17	
	whole hippocampus	0.47	7.3e-07	7.7e-06	**
thalamus subregions	mediodorsal	-0.36	3.3e-05	0.00015	**
	ventral lateral	-0.30	1.3e-04	0.00046	**
	lateral posterior	0.22	1.8e-02	0.047	*
	lateral geniculate	0.37	9.1e-05	0.00038	**
	medial ventral (reuniens)	0.39	1.1e-04	0.00042	**
hippocampus subregions	GC ML DG	0.41	1.4e-05	7.3e-05	**
	CA4	0.42	9.8e-06	5.9e-05	**
	subiculum	0.47	1.3e-07	1.9e-06	**
	CA1	0.48	3.9e-06	2.8e-05	**
	molecular layer	0.49	1.2e-06	1e-05	**
	hippocampal fissure	0.54	2.2e-08	4.7e-07	**
	hippocampal tail	0.61	1.4e-09	5.9e-08	**
amygdala subregions	accessory basal nucleus	0.21	1.9e-02	0.048	*
	paralaminal nucleus	0.28	1.8e-03	0.005	*
	basal nucleus	0.31	4.5e-04	0.0014	**

Generalized additive mixed models (GAMMs) linearly predicting normalized brain volumes from gene dosage (22qDel = 1, TD = 2, 22qDup = 3), controlling for sex, site, participant, and non-linear age effects. Gene dosage was positively related to total intracranial volume (ICV; all other models control for ICV), and whole hippocampus volume, but not to the whole thalamus or amygdala. Bi-directional effects within the thalamus and localized amygdala effects were observable at the subregion level. Gene dosage was negatively related to volume for thalamic mediodorsal and ventral lateral regions. All other subregions of the thalamus, hippocampus, or amygdala with significant effects exhibited positive relationships between gene dosage and volume. Results are presented for all whole structure volumes (whole thalamus, amygdala, hippocampus, and total intracranial volume), and for subregions with significant type I error corrected gene dosage effects. In the "sig" column, one star "*" indicates False Discovery Rate (FDR) $q < 0.05$, and two stars "**" indicate both FDR significance and significance at Bonferroni adjusted $\alpha < 0.05$.

GC granule cell, ML molecular layer, DG dentate gyrus, CA cornu ammonis.

or Siemens Prisma scanner with the same T1-weighted (T1w) sequence [33]. Scan sessions at all timepoints were first processed cross-sectionally using the recon-all anatomical segmentation pipeline in FreeSurfer 7.3.2 [34,35]. The FreeSurfer longitudinal stream was subsequently applied, which has been shown to significantly improve reliability and statistical power in repeated measure analyses [36].

Subcortical nuclei. For each scan, volume was estimated for the whole thalamus, amygdala, and hippocampus, and their subregions using Bayesian methods to automatically segment T1w images using template atlases based on histological data and ultra-high-resolution ex vivo MRI [37–40]. These segmentations are well-validated and have been applied by multiple consortia to large scale neuroimaging analyses [41–45]. See Supplementary Fig. S2 for visualization of the FreeSurfer segmentation and Supplementary Methods for a list of all regions analyzed as well as details on segmentation, qualitative and statistical quality control (QC) procedures, and between-scanner harmonization using longitudinal ComBat [46].

Gene dosage and maturational effects. To investigate the linear effect of CNV status on subcortical volumes, and to capture the non-linear relationship between age and volume, we used a generalized additive mixed model (GAMM) with a linear fixed effect for gene dosage, which was numerically coded by CNV status: 22qDel = 1, TD = 2, and 22qDup = 3 copies of the 22q11.2 locus. Age was modeled with separate thin plate regression splines in each group [47], restricted to exactly 2 degrees of freedom to facilitate comparison [48]. GAMMs are a nonlinear extension of mixed effects regression, allowing for repeat visits to be modeled with a random intercept [49]. Biological sex and site were also included as fixed effects. Total intracranial volume (ICV) was included as a fixed effect in all models except where ICV was the dependent variable. ComBat-adjusted volumes for each region were normalized based on the TD mean and standard deviation.

Gene dosage effects were tested for total ICV, whole thalamus, hippocampus, and amygdala volumes, and 38 subregions. All tests were corrected for multiple comparisons using the standard False Discovery Rate (FDR) at a threshold of $q < 0.05$ across the 42 volumes [50].

To characterize maturational trajectories, p -values for the non-linear effect of age in each group were computed and evaluated at $q < 0.05$ across all 126 models. Age ranges of significant difference between CNV groups and controls were computed from the 95% confidence interval for the difference in curves.

Secondary analyses. Regional volume differences compared to the TD group were tested separately for 22qDel and 22qDup groups. Gene dosage analyses were also repeated without averaging structures bilaterally, to detect any asymmetric hemispheric effects. Secondary analyses of the interaction between sex and gene dosage on brain volumes were also tested. The effect of antipsychotic medication was also investigated.

Cognition and symptom analyses. Motivated by literature relating low hippocampal tail volume to verbal learning impairment in 22qDel [27], we assessed verbal and non-verbal IQ [Wechsler Abbreviated Scale of Intelligence (WASI-2) Vocabulary and Matrix subtest scaled scores] for associations with hippocampal tail volume in each group. Given the relationship between 22qDel and psychosis risk [9, 26, 51], we additionally tested relationships between psychosis risk symptoms and all subcortical volumes in the 22qDel group.

RESULTS

Gene dosage effects

Total ICV was positively related to gene dosage (Table 2, Fig. 1). All other models controlled for ICV. Positive gene dosage effects on

Volume Predicted by Gene Dosage

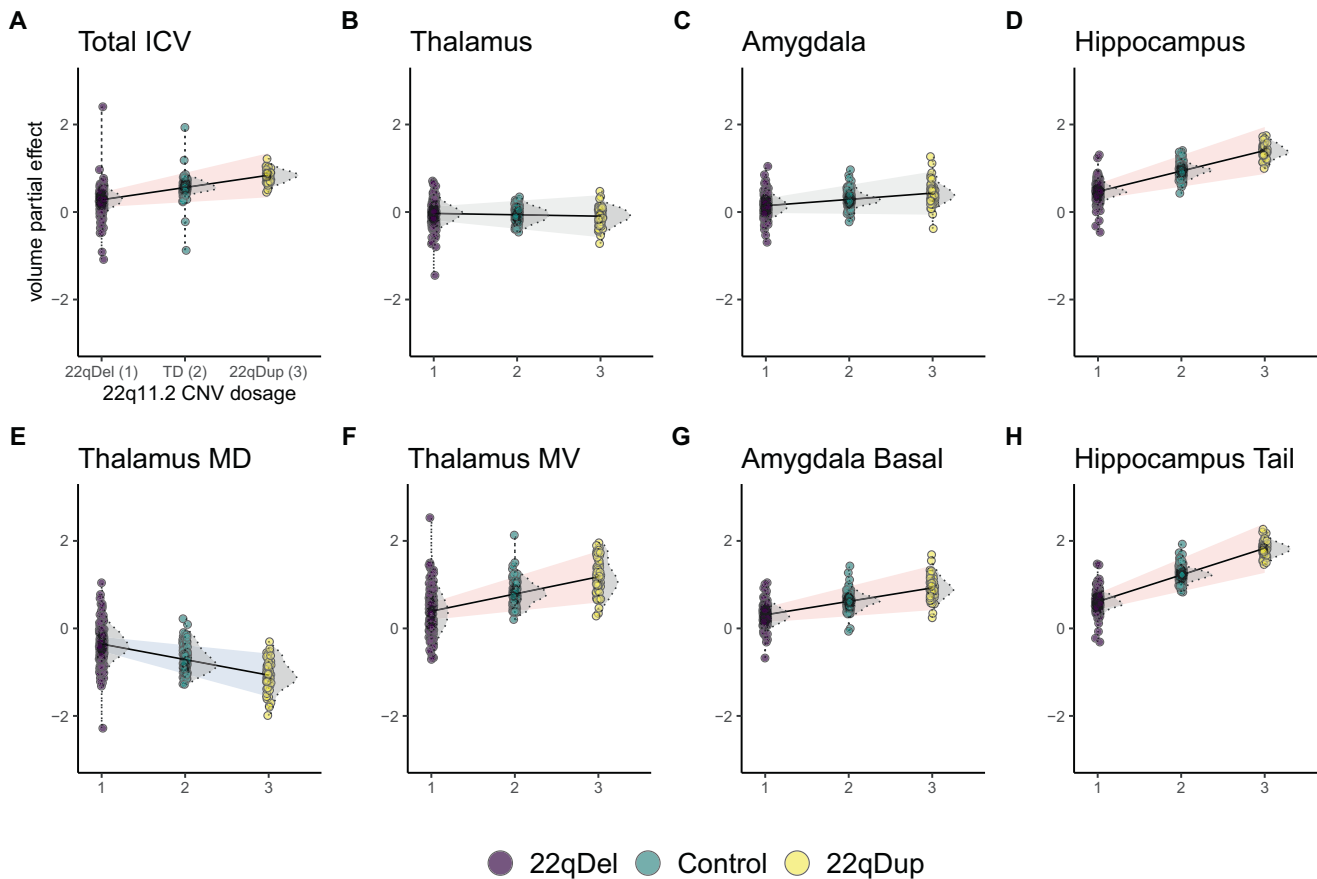


Fig. 1 Visualization of gene dosage effects on selected volumes. Estimated linear partial effects of gene dosage on volume with 95% confidence intervals (CI) for the estimate. Red CI indicates significant positive gene dosage relationship (False Discovery Rate $q < 0.05$), blue indicates significant negative relationship, and gray indicates no relationship. Partial residual scatterplots are shown for 22qDel (purple) control (green) and 22qDup (yellow), with kernel density estimates for each group in gray. **A** Total intracranial volume (ICV). All other models control for ICV. **B–D** There was a significant positive relationship between gene dosage and whole hippocampus volume, which was not observed for the thalamus or amygdala. **E, F** Within the thalamus, some subregions (e.g., MD; mediadorsal) showed negative gene dosage-volume relationships, while others (e.g., MV; medial ventral) exhibited positive effects. **G** Several amygdala subregions (e.g., basal nucleus) exhibited positive gene dosage effects, despite the whole amygdala having no relationship between gene dosage and volume. **H** Significant hippocampal subregions (e.g., hippocampal tail) had the same direction of effect as the whole hippocampus.

volume were observed for the whole hippocampus, but not the whole thalamus or amygdala.

Within the thalamus and amygdala, individual subregions showed significant gene dosage effects (Table 2, Fig. 1). There were bi-directional gene dosage effects on thalamic volumes; negative gene dosage effects were observed for the mediadorsal and ventral lateral nuclei, while positive gene dosage effects were observed in the lateral posterior, lateral geniculate, and reuniens nuclei. Within the amygdala, positive gene dosage effects were observed for the accessory basal, paralaminar, and basal nuclei. Multiple hippocampal subregions exhibited positive gene dosage effects in line with the whole structure findings, with the strongest effect in the hippocampal tail.

Maturational effects. GAMM analysis revealed multiple subcortical regions with significant age-related changes in each cohort (Fig. 2, 3 and Table S5). Overall, 22qDel and TD cohorts exhibited age-related changes across various subregions in the thalamus, hippocampus, and amygdala, while in 22qDup, age-related changes were only detected in thalamic regions and the hippocampal tail. All three groups exhibited significant age-related decreases in thalamic medial geniculate volumes, but medial geniculate volumes in 22qDup increased slightly after

approximately age 30, whereas in the other groups they continued to decrease. Developmental trajectories after age 30 should be interpreted with caution, though, due to the lower number of participants in this age range. For this reason, we repeated the maturational analyses in a subset of participants under 35 years of age (Figs. S4–7), finding broadly similar patterns to those observed in the analyses including the full age range.

Several regions exhibited significant age-related changes in only CNV carriers, but not TD controls (Fig. 2). The anteroventral thalamus showed age effects in only 22qDel, involving steeper decreases in childhood and adolescence compared to the other groups (Fig. 3). Ventral anterior thalamus results were similar. Medial ventral and laterodorsal thalamus showed significant age effects in only 22qDup, but the curves overlapped TD at all ages. Several hippocampus and amygdala subregions exhibited significant age effects in TD controls but neither CNV group. In the hippocampal CA2/3 and CA4 regions, TD controls exhibited an inverted-U-shaped developmental curve, which was mostly flattened in 22qDel and 22qDup (Fig. 3). CA2/3 volumes in 22qDel were greater than TD between ages 5.5–8.8 and lower than TD between ages 14.7–26.1, with similar periods of difference for 22qDup versus TD (Table S5).

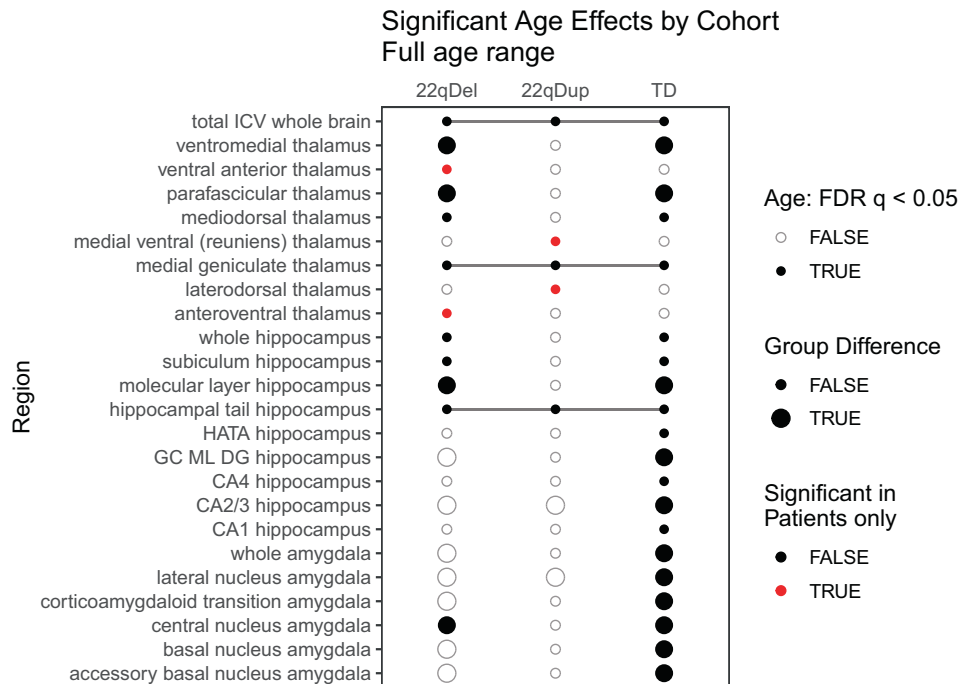


Fig. 2 Summary of age effects on subcortical volumes. For each group, regions with FDR-corrected significant age effects on volume ($q < 0.05$) are marked with a dark circle. Large circles indicate at least one age range with a significant difference between CNV patients (22qDel or 22qDup) and TD control age curves based on the 95% confidence interval (CI), whereas small circles indicate overlapping patient and control curves. Red circles indicate regions where the smoothed effect of age is significant in either patient group but not controls. Lines connect regions with significant age effects in all three groups. See Supplementary Fig. S5 for results of the same GAMMs restricted to participants under 35 years of age.

Secondary analyses

When tested in separate case-control analyses, 14 regions showed significant effects of 22qDel versus TD (Table S2), and one region (mediodorsal thalamus) showed a significant effect of 22qDup versus TD (Table S3), at a threshold of $q < 0.05$ across the 86 tests across both groups.

Secondary analyses of separate left and right hemispheres showed strong concordance in gene dosage effects on regional volumes across both hemispheres (Table S4). Significant main effects of sex on subcortical volumes were found for 27 regions (see Table S6). However, no significant interactions were found with gene dosage. Additionally, when the gene dosage analysis was repeated with the addition of a covariate for antipsychotic medication status, the results were highly comparable to the primary analysis (Table S7).

Cognition and symptom analyses. Hippocampal tail volume in 22qDel was significantly associated with Verbal IQ ($\beta = 1.86$, $p = 0.011$) but not Nonverbal IQ; however, no relationships were observed in the 22qDup or TD groups. See Fig. S3 for scatter plots and p -values in all groups.

No subcortical regions were found to exhibit significant relationships between volume and either continuous or categorical measures of positive psychosis-risk symptoms in the 22qDel group. In the 22qDel group, no subcortical regions exhibited a significant relationship between antipsychotic medication status and volume.

DISCUSSION

This is the first study to systematically characterize the relationship between the dosage of genomic material at the 22q11.2 locus and the volumes of specific subcortical nuclei. It is also the first study to investigate longitudinal subcortical development in 22qDup. We used an accelerated longitudinal design to recruit an

unprecedented sample of 22qDel and 22qDup carriers and TD controls, spanning from childhood to middle adulthood. Using linear and nonlinear mixed effects regression approaches to map gene dosage and age effects on regional volumes, we identified several novel findings, specifically: (1) gene dosage at the 22q11.2 locus is positively related to total intracranial and hippocampal volume, but not whole thalamus or amygdala volume; (2) 22q11.2 gene dosage has positive relationships to specific amygdala subregions, and bi-directional relationships to specific thalamic nuclei; and, (3) longitudinal development of subcortical structures is differentially altered in 22qDel and 22qDup across subcortical regions.

Gene dosage effects

Standardized beta effect sizes for gene dosage effects on volume were of similar magnitude to effect sizes from previous large studies of cortical and subcortical brain structure in neurodevelopmental CNVs including 22qDel [3, 19] and idiopathic neurodevelopmental and psychiatric disorders [23, 24]. For example, hippocampal volume was found to be -0.46 standard deviations in patients with schizophrenia compared to controls [24], compared to our whole hippocampus effect size of -0.85 standard deviations between 22qDel and TD (Table S2). Case-control effect sizes were somewhat smaller in 22qDup versus TD, with the single significant region (mediodorsal thalamus; Table S3), exhibiting an effect size of -0.44 .

These findings extend prior work from Lin et al., who provided the first evidence for a gene dosage relationship to cortical thickness, surface area, ICV, and hippocampal volume in individuals with reciprocal 22q11.2 CNVs [18]. Anatomical subregions were not investigated in that study, but a shape analysis suggested that these structures may be non-uniformly impacted. In that analysis, hippocampal thickness was found to be greater in 22qDup relative to 22qDel in regions roughly corresponding to the subiculum and CA1, which is corroborated

Developmental Trajectories Full age range

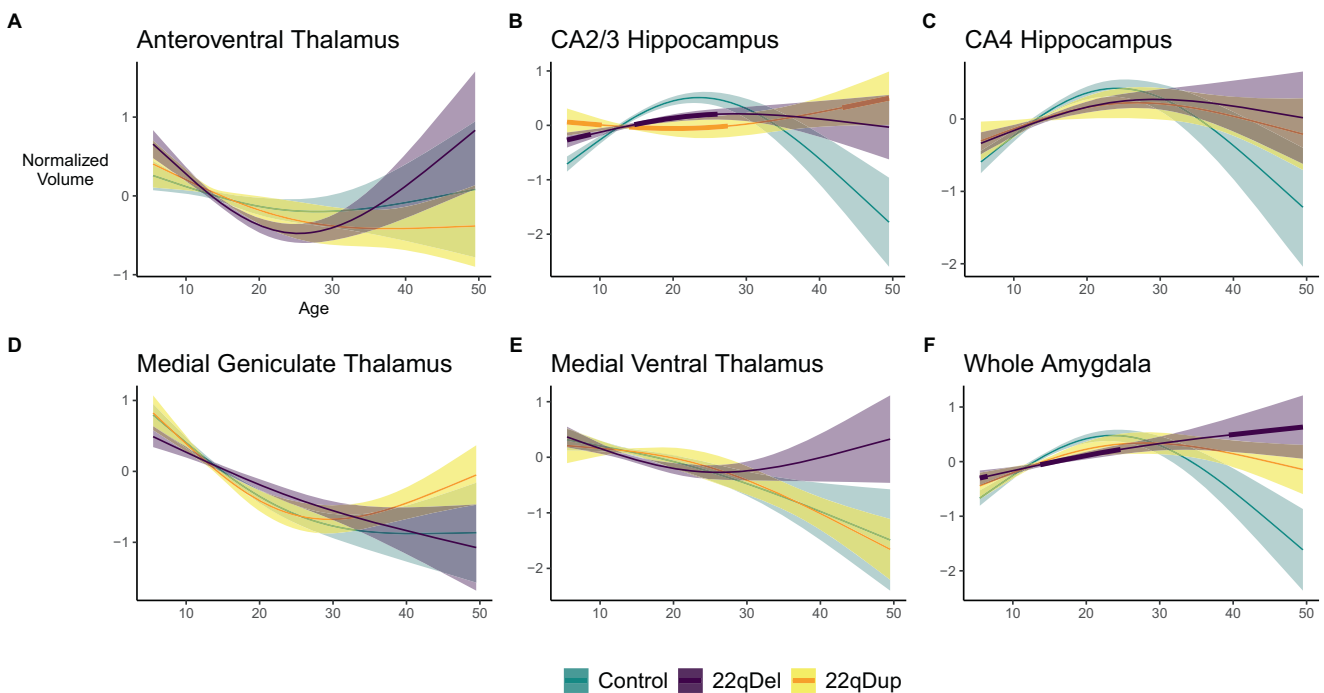


Fig. 3 Selected age curves. GAMMs in 22qDel (purple), 22qDup (yellow/orange), and TD controls (green), showing the relationship between age and selected subregion volumes, controlling for covariates. Thick lines in the 22qDel and 22qDup curves indicate age ranges of significant difference from controls based on the 95% confidence interval. **A** 22qDel experience steeper early life declines in anteroventral thalamus volume. **B, C** In the hippocampal CA2/3 and CA4 regions, TD controls exhibit an inverted-U-shaped developmental curve, which is mostly flattened in both 22qDel and 22qDup. CA2/3 volumes in 22qDel and 22qDup were greater than TD in childhood, lower in early to middle adulthood, and potentially higher in later adulthood. **D** All groups show significant age-related decreases in medial geniculate thalamus volumes. **E** Medial ventral (reuniens) thalamus development is similar between groups, especially in childhood through early adulthood, but only 22qDup show a significant age effect. **F** 22qDel whole amygdala development is flattened compared to controls. See Supplementary Fig. S4 for the same curves with scatterplots of partial residuals for each participant, and Supplementary Figs. S6–7 for GAMMs restricted to participants under age 35.

by our current study. However, our approach did not find any regions of decreased hippocampal volume in 22qDup relative to 22qDel, whereas Lin et al. found support for some localized thickness decreases in 22qDup in regions approximately corresponding to CA2–4. Here, we expand on and broadly replicate the previous hippocampal findings in this larger longitudinal sample and have increased sensitivity to detect effects localized to specific nuclei.

Notably, within the thalamus we found bi-directional gene dosage effects across subregions. Volumes of the mediodorsal and ventral lateral nuclei decreased with increasing 22q11.2 copy number, whereas the opposite was observed for the lateral posterior, lateral geniculate and reuniens nuclei. Contrary to our hypothesis, the bi-directional effects did not follow a sensory/executive pattern; both the mediodorsal and reuniens nuclei have strong connections to the prefrontal cortex, whereas the ventral lateral, lateral posterior and lateral geniculate nuclei are more strongly connected to motor and visual cortex [52–54]. Interestingly, the reuniens nucleus, which exhibited the strongest thalamic effects, is a key hub in a network connecting the thalamus, hippocampus, and prefrontal cortex [55–57]. In 22qDel, bi-directional disruptions have been observed in functional connectivity of the thalamus and hippocampus to regions including the prefrontal cortex [58].

Analysis of hippocampal tail volume relationships to IQ suggests that this region may be particularly related to verbal cognition in 22qDel, but not 22qDup or TD. This broadly supports the recent finding of hippocampal tail volume relationships with verbal

learning scores in 22qDel [27]. Our analysis was specifically motivated by this prior literature; however, this effect would not have remained significant after correction for multiple comparisons in an exploratory analysis of cognition relationships to all subregional volumes.

Exploratory analyses did not find significant psychosis-risk symptom/volume relationships. However, a large multi-site study of subcortical volumes in 22qDel did find evidence for lower thalamus, hippocampus, and amygdala volumes in 22qDel individuals with psychotic disorder, compared to those without [19]. This suggests that, within the 22qDel population decreased subcortical volumes may only be detectable in those meeting full criteria for psychotic disorder, rather than subthreshold symptomatology. The current 22qDel sample was only powered to test psychosis-risk associations (Table 1).

Maturational effects. Studies of normative subcortical development often show volume increases in childhood followed by decreases later in life, and this pattern is particularly prominent in the hippocampus and amygdala [59–61]. We find that in hippocampal CA2/3, and to a lesser extent CA4, both 22qDel and 22qDup failed to exhibit the expected early life increases and adult decreases observed in TD. This was not observable in the whole hippocampus, where curves overlapped across the age range. Amygdala volumes in the three groups followed more similar developmental trajectories, except that in 22qDel volumes continued to increase in adulthood, while plateauing or decreasing in the other groups. All groups exhibited similar age-related

decreases across many thalamic subregions. These trajectories were more linear compared to the hippocampus and amygdala. 22qDel had abnormally steep decreases in anteroventral thalamic volumes, a thalamic subregion implicated in spatial learning and memory [62]. The steep declines in 22qDel anteroventral thalamus volumes may reflect either an abnormal developmental mechanism, or compensatory changes related to the abnormally high volume in early childhood. A prior independent longitudinal study of 22qDel and TD using a similar thalamic parcellation found an overall pattern of age-related volume decreases resembling many of the thalamic age effects in our current study [26]. However, that study used linear models rather than nonlinear splines, and as such was not sensitive to differential rates of change across different age periods, which we observe for certain regions.

Our analyses of maturational trajectories build on recent longitudinal cortical findings of altered developmental trajectories of cortical thickness and surface area in 22q11.2 CNVs [47]. Jalbrzikowski et al. found that 22qDel, 22qDup, and TD controls all showed broad decreases in cortical thickness from childhood to adulthood, but the 22qDel group showed a protracted pattern of cortical thinning. 22qDup did not exhibit the same age-related cortical surface area decreases observed in TD and 22qDel.

Relationship to post-mortem human and animal model findings

The approach of mapping gene dosage effects on MRI-derived volumes to histologically-defined subcortical nuclei allows for more effective comparison between our neuroimaging results and findings from post-mortem brain tissue.

The strongest negative gene dosage effects were in the mediodorsal thalamus, a major source of thalamic input to the prefrontal cortex. This region has been highly studied in post-mortem brain tissue from individuals with schizophrenia, but findings are mixed, with several reporting decreased volumes and cell counts, and others reporting no differences to controls [29]. The strong effect we observe on this structure in 22q11.2 CNVs suggests a particular disruption of thalamic-prefrontal development that may be distinct from the changes underlying most idiopathic schizophrenia cases. Studies of the hippocampus in schizophrenia have demonstrated reductions in the volume and/or neuron number in subfields including the subiculum, CA1, CA2/3, and CA4 [63], which are consistent with our findings of decreased hippocampal volumes in 22qDel patients who are at increased risk for schizophrenia, compared to 22qDup who are at lower risk [14–16].

Subregion-specific analysis also helps connect results to animal model findings, which are often reported relative to these histological regions. Mouse models of 22qDel have repeatedly shown disruption to structure, function, and development of hippocampal regions CA1, CA2 and CA3 [64–66]. GABAergic inhibitory cells are particularly implicated in these disruptions. Alterations in thalamic-cortical functional connectivity in 22qDel mice have been related to changes in the auditory thalamus mediated by microRNA processes downstream of the 22q11.2 gene *Dgcr8*, which have been corroborated in human post-mortem tissue from individuals with schizophrenia [67]. *Dgcr8* haploinsufficiency has also been linked to decreased dendritic spine density in regions including hippocampal CA1 in a 22qDel mouse model [68].

Strengths, limitations, and future directions. Several strengths of this study should be considered in support of its reliability. The sample size of 191 scans from 96 participants with 22qDel, and 64 scans from 37 individuals with 22qDup is large for rare genetic disorders [69]. The 22qDup neuroimaging sample is unprecedented in size for that syndrome. Our large sample of 22q11.2 CNV carriers and TD controls spans a wide age range, allowing us to test important developmental hypotheses. However, the age

distributions are right-skewed, and the data spanning middle adulthood were limited.

Our unique sample with identically acquired structural images from individuals with 22qDel, 22qDup, and TD controls allows for a powerful regression analysis approach in which approximate 22q11.2 gene dosage is operationalized as an integer value. This allows us to go beyond case-control differences to test specifically for brain phenotypes that are related to the content of genomic material in these reciprocal CNVs. While each carrier had a molecularly confirmed CNV at the 22q11.2 locus, breakpoints can vary in some cases [7]. However, breakpoints at this locus are largely consistent due to the pattern of low copy repeats flanking the region [9]. Breakpoint variation is thus not expected to strongly influence results. Gene dosage also likely does not fully reflect differences in gene transcription and translation in brain tissue, which are likely more closely linked to phenotypes, but cannot be measured *in vivo* or inferred from less invasively collected tissue such as blood [70, 71]. Rather than solely focusing on case-control differences, the gene dosage effects detected by our model specifically represent instances where linear variations in the approximate gene dosage are predictive of significant variation in regional volume. When tested in separate case-control analyses, 22qDel carriers show somewhat stronger effects on subcortical structures relative to TD than do 22qDup, which is consistent with the more severe neurobehavioral/cognitive phenotype in 22qDel [13, 69, 72]. The smaller 22qDup sample size may partially explain the finding of fewer statistically significant differences between 22qDup and TD compared to 22qDel and TD (Tables S2 and S3). While the differences between 22qDel and the other two groups may be driving some of the gene dosage findings, the results of the primary gene dosage models along with the supplemental case-control analyses are highly informative, highlighting that the overall trend for subcortical regions is towards linear gene dosage relationships to volume, rather than convergent effects in 22qDel and 22qDup. In other words, there are no regions for which 22qDel and 22qDup significantly differ from TD in the same direction.

Future directions of research include characterization of gene dosage effects in other reciprocal CNVs such as the 16p11.2 and 15q11-q13 loci and mapping subcortical development in individuals with idiopathic autism and those at clinical high risk (CHR) for psychosis to determine convergent (and/or divergent) patterns. Larger multi-site studies of 22q11.2 CNVs will be better-powered to elucidate possible roles of breakpoint variation, and brain-behavior relationships. Analysis of cytoarchitecture and gene expression in post-mortem tissue from individuals with 22q11.2 CNVs will also be highly informative. Research in animal and *in vitro* models will continue to bridge the gap to understanding circuit-level dysfunction, and the roles of individual genes and potential targeted pharmacological interventions.

CONCLUSIONS

This study is the first to characterize gene dosage effects on subregional subcortical volumes in individuals with reciprocal 22q11.2 CNVs, and the first study of longitudinal development of subcortical structures in 22qDup. Using a linear mixed effects approach, we found positive gene dosage effects on total brain volume, hippocampal volumes, and several amygdala subregions, and bi-directional effects across multiple thalamic nuclei. GAMM analyses revealed both distinct and convergent disruptions in developmental trajectories in 22q11.2 CNVs across the thalamus, hippocampus, and amygdala. These results highlight the impact of genes in the 22q11.2 locus on subcortical brain development and motivate future research linking gene expression to brain phenotypes at the levels of cells, circuits, and macro-scale structures.

DATA AVAILABILITY

Data are publicly available from the National Institute of Mental Health Data Archives: https://nda.nih.gov/edit_collection.html?id=2414. To facilitate reproducibility and rigor, all analysis code is publicly available on GitHub: https://github.com/charles-schleifer/22q_subcort_volumes. A pre-print of this manuscript prior to peer review is hosted on bioRxiv: <https://doi.org/10.1101/2023.10.31.564553>.

REFERENCES

- Hoeffding LK, Trabjerg BB, Olsen L, Mazin W, Sparsø T, Vangkilde A, et al. Risk of psychiatric disorders among individuals with the 22q11.2 deletion or duplication: a Danish nationwide, register-based study. *JAMA Psychiatry*. 2017;74:282–90.
- Chawner SJRA, Doherty JL, Anney RJL, Antshel KM, Bearden CE, Bernier R, et al. A genetics-first approach to dissecting the heterogeneity of autism: phenotypic comparison of autism risk copy number variants. *Am J Psychiatry*. 2021;178:77–86.
- Moreau CA, Ching CR, Kumar K, Jacquemont S, Bearden CE. Structural and functional brain alterations revealed by neuroimaging in CNV carriers. *Curr Opin Genet Dev*. 2021;68:88–98.
- Provenzani U, Damiani S, Bersano I, Singh S, Moschillo A, Accinni T, et al. Prevalence and incidence of psychotic disorders in 22q11.2 deletion syndrome: a meta-analysis. *Int Rev Psychiatry*. 2022;34:676–88.
- Weisman O, Guri Y, Gur RE, McDonald-McGinn DM, Calkins ME, Tang SX, et al. Subthreshold psychosis in 22q11.2 deletion syndrome: multisite naturalistic study. *Schizophr Bull*. 2017;43:1079–89.
- Girirajan S, Brkanac Z, Coe BP, Baker C, Vives L, Vu TH, et al. Relative burden of large CNVs on a range of neurodevelopmental phenotypes. *PLoS Genet*. 2011;7:e1002334.
- Morrow BE, McDonald-McGinn DM, Emanuel BS, Vermeesch JR, Scambler PJ. Molecular genetics of 22q11.2 deletion syndrome. *Am J Med Genet A*. 2018;176:2070–81.
- Sayal K, Prasad V, Daley D, Ford T, Coghill D. ADHD in children and young people: prevalence, care pathways, and service provision. *Lancet Psychiatry*. 2018;5:175–86.
- McDonald-McGinn DM, Sullivan KE, Marino B, Philip N, Swillen A, Vorstman JAS, et al. 22q11.2 deletion syndrome. *Nat Rev Dis Prim*. 2015;1:15071.
- Ou Z, Berg JS, Yonath H, Enciso VB, Miller DT, Picker J, et al. Microduplications of 22q11.2 are frequently inherited and are associated with variable phenotypes. *Genet Med J Am Coll Med Genet*. 2008;10:267–77.
- Ensenauer RE, Adeyinka A, Flynn HC, Michels VV, Lindor NM, Dawson DB, et al. Microduplication 22q11.2, an emerging syndrome: clinical, cytogenetic, and molecular analysis of thirteen patients. *Am J Hum Genet*. 2003;73:1027–40.
- Portnoi M-F. Microduplication 22q11.2: a new chromosomal syndrome. *Eur J Med Genet*. 2009;52:88–93.
- Lin A, Vajdi A, Kushan-Wells L, Helleman G, Hansen LP, Jonas RK, et al. Reciprocal copy number variations at 22q11.2 produce distinct and convergent neurobehavioral impairments relevant for schizophrenia and autism spectrum disorder. *Biol Psychiatry*. 2020;88:260–72.
- Marshall CR, Howrigan DP, Merico D, Thiruvahindrapuram B, Wu W, Greer DS, et al. Contribution of copy number variants to schizophrenia from a genome-wide study of 41,321 subjects. *Nat Genet*. 2017;49:27–35.
- Rees E, Kirov G, Sanders A, Walters JTR, Chambert KD, Shi J, et al. Evidence that duplications of 22q11.2 protect against schizophrenia. *Mol Psychiatry*. 2014;19:37–40.
- Rees E, Walters JTR, Georgieva L, Isles AR, Chambert KD, Richards AL, et al. Analysis of copy number variations at 15 schizophrenia-associated loci. *Br J Psychiatry J Ment Sci*. 2014;204:108–14.
- Sun D, Ching CRK, Lin A, Forsyth JK, Kushan L, Vajdi A, et al. Large-scale mapping of cortical alterations in 22q11.2 deletion syndrome: convergence with idiopathic psychosis and effects of deletion size. *Mol Psychiatry*. 2020;25:1822–34.
- Lin A, Ching CRK, Vajdi A, Sun D, Jonas RK, Jalbrzikowski M, et al. Mapping 22q11.2 gene dosage effects on brain morphometry. *J Neurosci*. 2017;37:6183–99.
- Ching CRK, Gutman BA, Sun D, Villalon Reina J, Ragothaman A, Isaev D, et al. Mapping subcortical brain alterations in 22q11.2 deletion syndrome: effects of deletion size and convergence with idiopathic neuropsychiatric illness. *Am J Psychiatry*. 2020;177:589–600.
- Forstmann BU, de Hollander G, van Maanen L, Alkemade A, Keuken MC. Towards a mechanistic understanding of the human subcortex. *Nat Rev Neurosci*. 2017;18:57–65.
- Kumar K, Modenato C, Moreau C, Ching CRK, Harvey A, Martin-Brevet S, et al. Subcortical brain alterations in carriers of genomic copy number variants. *Am J Psychiatry*. 2023;180:685–98.
- Hibar DP, Stein JL, Renteria ME, Arias-Vasquez A, Desrivieres S, Jahanshad N, et al. Common genetic variants influence human subcortical brain structures. *Nature*. 2015;520:224–9.
- Boedhoe PSW, van Rooij D, Hoogman M, Twisk JWR, Schmaal L, Abe Y, et al. Subcortical brain volume, regional cortical thickness and cortical surface area across attention-deficit/hyperactivity disorder (ADHD), autism spectrum disorder (ASD), and obsessive-compulsive disorder (OCD). *Am J Psychiatry*. 2020;177:834–43.
- van Erp TGM, Hibar DP, Rasmussen JM, Glahn DC, Pearlson GD, Andreassen OA, et al. Subcortical brain volume abnormalities in 2028 individuals with schizophrenia and 2540 healthy controls via the ENIGMA consortium. *Mol Psychiatry*. 2016;21:547–53.
- Sherman SM. The thalamus is more than just a relay. *Curr Opin Neurobiol*. 2007;17:417–22.
- Mancini V, Zöllner D, Schneider M, Schaer M, Eliez S. Abnormal development and dysconnectivity of distinct thalamic nuclei in patients with 22q11.2 deletion syndrome experiencing auditory hallucinations. *Biol Psychiatry Cogn Neurosci Neuroimaging*. 2020;5:875–90.
- Latrèche C, Maeder J, Mancini V, Bortolin K, Schneider M, Eliez S. Altered developmental trajectories of verbal learning skills in 22q11.2DS: associations with hippocampal development and psychosis. *Psychol Med*. 2023;53:4923–32.
- Mancini V, Saleh MG, Delavari F, Bagautdinova J, Eliez S. Excitatory/inhibitory imbalance underlies hippocampal atrophy in individuals with 22q11.2 deletion syndrome with psychotic symptoms. *Biol Psychiatry*. 2023. <https://doi.org/10.1016/j.biopsych.2023.03.021>.
- Dorph-Petersen K-A, Lewis DA. Postmortem structural studies of the thalamus in schizophrenia. *Schizophr Res*. 2017;180:28–35.
- Steiner J, Brisch R, Schiltz K, Dobrowolny H, Mawrin C, Krzyżanowska M, et al. GABAergic system impairment in the hippocampus and superior temporal gyrus of patients with paranoid schizophrenia: a post-mortem study. *Schizophr Res*. 2016;177:10–17.
- Fiksinski AM, Hoftman GD, Vorstman JAS, Bearden CE. A genetics-first approach to understanding autism and schizophrenia spectrum disorders: the 22q11.2 deletion syndrome. *Mol Psychiatry*. 2023;28:341–53.
- Forsyth JK, Mennigen E, Lin A, Sun D, Vajdi A, Kushan-Wells L, et al. Prioritizing genetic contributors to cortical alterations in 22q11.2 deletion syndrome using imaging transcriptomics. *Cereb Cortex*. 2021;31:3285–98.
- Jack CR Jr, Bernstein MA, Fox NC, Thompson P, Alexander G, Harvey D, et al. The Alzheimer's disease neuroimaging initiative (ADNI): MRI methods. *J Magn Reson Imaging*. 2008;27:685–91.
- Fischl B, Salat DH, Busa E, Albert M, Dieterich M, Haselgrove C, et al. Whole brain segmentation: automated labeling of neuroanatomical structures in the human brain. *Neuron*. 2002;33:341–55.
- Fischl B, van der Kouwe A, Destrieux C, Halgren E, Ségonne F, Salat DH, et al. Automatically parcellating the human cerebral cortex. *Cereb Cortex*. 2004;14:11–22.
- Reuter M, Schmansky NJ, Rosas HD, Fischl B. Within-subject template estimation for unbiased longitudinal image analysis. *Neuroimage*. 2012;61:1402–18.
- Iglesias JE, Augustinack JC, Nguyen K, Player CM, Player A, Wright M, et al. A computational atlas of the hippocampal formation using ex vivo, ultra-high resolution MRI: application to adaptive segmentation of in vivo MRI. *Neuroimage*. 2015;115:117–37.
- Iglesias JE, Van Leemput K, Augustinack J, Insausti R, Fischl B, Reuter M, et al. Bayesian longitudinal segmentation of hippocampal substructures in brain MRI using subject-specific atlases. *Neuroimage*. 2016;141:542–55.
- Iglesias JE, Insausti R, Lerma-Usabiaga G, Bocchetta M, Van Leemput K, Greve DN, et al. A probabilistic atlas of the human thalamic nuclei combining ex vivo MRI and histology. *Neuroimage*. 2018;183:314–26.
- Saygin ZM, Kliemann D, Iglesias JE, van der Kouwe AJW, Boyd E, Reuter M, et al. High-resolution magnetic resonance imaging reveals nuclei of the human amygdala: manual segmentation to automatic atlas. *Neuroimage*. 2017;155:370–82.
- Sämann PG, Iglesias JE, Gutman B, Grotegerd D, Leenings R, Flint C, et al. FreeSurfer-based segmentation of hippocampal subfields: a review of methods and applications, with a novel quality control procedure for ENIGMA studies and other collaborative efforts. *Hum Brain Mapp*. 2022;43:207–33.
- Grace S, Rossetti MG, Allen N, Batalla A, Bellani M, Brambilla P, et al. Sex differences in the neuroanatomy of alcohol dependence: hippocampus and amygdala subregions in a sample of 966 people from the ENIGMA Addiction Working Group. *Transl Psychiatry*. 2021;11:156.
- Weeland CJ, Kasprzak S, de Joode NT, Abe Y, Alonso P, Ameis SH, et al. The thalamus and its subnuclei—a gateway to obsessive-compulsive disorder. *Transl Psychiatry*. 2022;12:70.

44. Huang AS, Rogers BP, Sheffield JM, Jalbrzikowski ME, Anticevic A, Blackford JU, et al. Thalamic nuclei volumes in psychotic disorders and in youths with psychosis spectrum symptoms. *Am J Psychiatry*. 2020;177:1159–67.
45. Hoang D, Lizano P, Lutz O, Zeng V, Raymond N, Miewald J, et al. Thalamic, amygdalar, and hippocampal nuclei morphology and their trajectories in first episode psychosis: a preliminary longitudinal study. *Psychiatry Res Neuroimaging*. 2021;309:111249.
46. Beer JC, Tustison NJ, Cook PA, Davatzikos C, Sheline YI, Shinohara RT, et al. Longitudinal ComBat: a method for harmonizing longitudinal multi-scanner imaging data. *NeuroImage*. 2020;220:117129.
47. Jalbrzikowski M, Lin A, Vajdi A, Grigoryan V, Kushan L, Ching CRK, et al. Longitudinal trajectories of cortical development in 22q11.2 copy number variants and typically developing controls. *Mol Psychiatry*. 2022;27:1–10.
48. Larsen B, Bourque J, Moore TM, Adebimpe A, Calkins ME, Elliott MA, et al. Longitudinal development of brain iron is linked to cognition in youth. *J Neurosci*. 2020;40:1810–8.
49. Hastie TJ. Generalized additive models. Statistical models in S. Routledge. New York. 1992.
50. Benjamini Y, Hochberg Y. Controlling the false discovery rate: a practical and powerful approach to multiple testing. *J R Stat Soc Ser B Methodol*. 1995;57:289–300.
51. Jalbrzikowski M, Lin A, Vajdi A, Grigoryan V, Kushan L, Ching CRK, et al. Longitudinal trajectories of cortical development in 22q11.2 copy number variants and typically developing controls. *Mol Psychiatry*. 2022;27:4181–90.
52. Georgescu IA, Popa D, Zagrean L. The anatomical and functional heterogeneity of the mediodorsal thalamus. *Brain Sci*. 2020;10:624.
53. Kosif R. The thalamus: a review of its functional anatomy. *Med Res Arch*. 2016;4:801.
54. McFarland NR, Haber SN. Thalamic relay nuclei of the basal ganglia form both reciprocal and nonreciprocal cortical connections, linking multiple frontal cortical areas. *J Neurosci*. 2002;22:8117–32.
55. Dolleman-van der Weel MJ, Griffin AL, Ito HT, Shapiro ML, Witter MP, Vertes RP, et al. The nucleus reuniens of the thalamus sits at the nexus of a hippocampus and medial prefrontal cortex circuit enabling memory and behavior. *Learn Mem*. 2019;26:191–205.
56. Ferraris M, Cassel J-C, Pereira de Vasconcelos A, Stephan A, Quilichini PP. The nucleus reuniens, a thalamic relay for cortico-hippocampal interaction in recent and remote memory consolidation. *Neurosci Biobehav Rev*. 2021;125:339–54.
57. Herkenham M. The connections of the nucleus reuniens thalami: evidence for a direct thalamo-hippocampal pathway in the rat. *J Comp Neurol*. 1978;177:589–609.
58. Schleifer C, Lin A, Kushan L, Ji JL, Yang G, Bearden CE, et al. Dissociable disruptions in thalamic and hippocampal resting-state functional connectivity in youth with 22q11.2 deletions. *J Neurosci J Soc*. 2019;39:1301–19.
59. Coupé P, Catheline G, Lanuza E, Manjón JV. Alzheimer's disease neuroimaging initiative. Towards a unified analysis of brain maturation and aging across the entire lifespan: a MRI analysis. *Hum Brain Mapp*. 2017;38:5501–18.
60. Bethlehem Ral, Seidlitz J, White SR, Vogel JW, Anderson KM, Adamson C, et al. Brain charts for the human lifespan. *Nature*. 2022;604:525–33.
61. Dima D, Modabbernia A, Papachristou E, Doucet GE, Agartz I, Aghajani M, et al. Subcortical volumes across the lifespan: data from 18,605 healthy individuals aged 3–90 years. *Hum Brain Mapp*. 2021;43:452–69.
62. Nelson AJD. The anterior thalamic nuclei and cognition: a role beyond space? *Neurosci Biobehav Rev*. 2021;126:1–11.
63. Roeske MJ, Konradi C, Heckers S, Lewis AS. Hippocampal volume and hippocampal neuron density, number and size in schizophrenia: a systematic review and meta-analysis of postmortem studies. *Mol Psychiatry*. 2021;26:3524–35.
64. Al-Absi A-R, Thambiappa SK, Khan AR, Glerup S, Sanchez C, Landau AM, et al. Df(h22q11)/+ mouse model exhibits reduced binding levels of GABAA receptors and structural and functional dysregulation in the inhibitory and excitatory networks of hippocampus. *Mol Cell Neurosci*. 2022;122:103769.
65. Piskowski RA, Nasrallah K, Diamantopoulou A, Mukai J, Hassan SI, Siegelbaum SA, et al. Age-dependent specific changes in area CA2 of the hippocampus and social memory deficit in a mouse model of the 22q11.2 deletion syndrome. *Neuron*. 2016;89:163–76.
66. Drew LJ, Stark KL, Fénelon K, Karayiorgou M, MacDermott AB, Gogos JA. Evidence for altered hippocampal function in a mouse model of the human 22q11.2 microdeletion. *Mol Cell Neurosci*. 2011;47:293–305.
67. Chun S, Du F, Westmoreland JJ, Han SB, Wang Y-D, Eddins D, et al. Thalamic miR-338-3p mediates auditory thalamocortical disruption and its late onset in models of 22q11.2 microdeletion. *Nat Med*. 2017;23:39–48.
68. Stark KL, Xu B, Bagchi A, Lai W-S, Liu H, Hsu R, et al. Altered brain microRNA biogenesis contributes to phenotypic deficits in a 22q11-deletion mouse model. *Nat Genet*. 2008;40:751–60.
69. Sønderby IE, Ching CRK, Thomopoulos SI, van der Meer D, Sun D, Villalon-Reina JE, et al. Effects of copy number variations on brain structure and risk for psychiatric illness: large-scale studies from the ENIGMA working groups on CNVs. *Hum Brain Mapp*. 2022;43:300–28.
70. Lin A, Forsyth JK, Hoftman GD, Kushan-Wells L, Jalbrzikowski M, Dokuru D, et al. Transcriptomic profiling of whole blood in 22q11.2 reciprocal copy number variants reveals that cell proportion highly impacts gene expression. *Brain Behav Immun Health*. 2021;18:100386.
71. Aguet F, Brown AA, Castel SE, Davis JR, He Y, Jo B, et al. Genetic effects on gene expression across human tissues. *Nature*. 2017;550:204–13.
72. O'Hara KP, Kushan-Wells L, Schleifer CH, Cruz S, Hoftman GD, Jalbrzikowski M, et al. Distinct neurocognitive profiles and clinical phenotypes associated with copy number variation at the 22q11.2 locus. *Autism Res*. 2023;16:2247–62.

AUTHOR CONTRIBUTIONS

Charles H. Schleifer: conceptualization, methodology, software, validation, formal analysis, data curation, writing - original draft, writing - review & editing, visualization; Kathleen P. O'Hara and Hoki Fung: data curation, methodology, writing - review & editing; Jenny Xu and Angela S. Wu: data curation, writing - review & editing; Taylor-Ann Robinson and Amy Lin: data curation; Leila Kushan-Wells: investigation, resources, data curation, project administration; Christopher R. K. Ching: conceptualization, writing - review & editing; Carrie E. Bearden: conceptualization, investigation, writing - review & editing, supervision, project administration, funding acquisition.

FUNDING

This work was supported by the National Institute of Mental Health Grant Nos. R01 MH085953 (to CEB), U01MH101779 (to CEB); the Simons Foundation (SFARI Explorer Award to CEB), and the Joanne and George Miller Family Endowed Term Chair (to CEB), the UCLA Training Program in Neurobehavioral Genetics T32NS048004 (to CHS), and the National Institute of Mental Health Grant F31MH133326-01 (to CHS)

COMPETING INTERESTS

The authors declare no competing interests.

ADDITIONAL INFORMATION

Supplementary information The online version contains supplementary material available at <https://doi.org/10.1038/s41386-024-01832-3>.

Correspondence and requests for materials should be addressed to Charles H. Schleifer or Carrie E. Bearden.

Reprints and permission information is available at <http://www.nature.com/reprints>

Publisher's note Springer Nature remains neutral with regard to jurisdictional claims in published maps and institutional affiliations.



Open Access This article is licensed under a Creative Commons Attribution 4.0 International License, which permits use, sharing, adaptation, distribution and reproduction in any medium or format, as long as you give appropriate credit to the original author(s) and the source, provide a link to the Creative Commons licence, and indicate if changes were made. The images or other third party material in this article are included in the article's Creative Commons licence, unless indicated otherwise in a credit line to the material. If material is not included in the article's Creative Commons licence and your intended use is not permitted by statutory regulation or exceeds the permitted use, you will need to obtain permission directly from the copyright holder. To view a copy of this licence, visit <http://creativecommons.org/licenses/by/4.0/>.

© The Author(s) 2024